

PACS numbers: 68.37.Hk, 81.05.ub, 81.15.Cd, 81.15.Gh, 84.60.Jt, 88.40.hj, 88.40.jj

## Determination of Output Power of Si–CNT Solar Cell

Z. B. Ibraheem<sup>1</sup>, M. M. Uonis<sup>1</sup>, and M. A. Abed<sup>2</sup>

<sup>1</sup>*College of Science,  
Department of New and Renewable Energy,  
Mosul University,  
Mosul, Iraq*

<sup>2</sup>*College of Science,  
Department of Physics,  
Mosul University,  
Mosul, Iraq*

Plasma-sputtering technique is used to deposit the carbon layers with different nanoscale thicknesses on the *p*-type silicon wafers. The scanning electron-microscope images show the grains' size growth and aggregation in clusters. The electrical properties of the junction behave as a solar cell, and this gives the proof of formation of the carbon nanotubes (CNT). Both the out power and the efficiency of the Si–CNT cells increase with carbon-layer thickness and light intensity.

Техніка плазмового напорошення використовується для нанесення вуглецевих шарів різної нанорозмірної товщини на *p*-типу кремнійові пластини. Зображення сканувального електронного мікроскопа показують зростання розмірів зерен і агрегацію їх у кластери. Електричні властивості переходу поведуться як сонячний елемент, і це дає доказ утворення вуглецевих нанотрубок (ВНТ). Як вихідна потужність, так і ефективність елементів Si–ВНТ зростають зі збільшенням товщини вуглецевого шару й інтенсивності світла.

**Key words:** carbon nanotube, solar cells, *p–n* junction.

**Ключові слова:** вуглецеві нанотрубки, сонячні елементи, *p–n*-перехід.

(Received 20 February, 2023; in revised form, 11 May, 2023)

### 1. INTRODUCTION

The importance of carbon as a chemical element comes from the

ability of its large atoms to bond with each other or with atoms of different chemical elements in different ways. This diversity in bonding gives a diversity of structural forms, including crystalline carbon such as graphite and fullerene, amorphous carbon and carbon nanoparticles, including carbon nanotubes, each of these shapes is characterized by different properties, including a low coefficient of friction, high thermal conductivity, optical transmittance, hardness, as well as being non-toxic or harmful to the environment. In 1985, Kroto and Smalley gave the name fullerene to clusters of carbon atoms that contain sixty carbon atoms  $C_{60}$ , which are a group of icosahedral symmetry closed molecules, and, because of the similarity between them and Buckminster's designs, R. Buckminster called them as 'buckminster fullerene', and for short, these molecules are called 'buckyballs' [1, 2].

Fullerene particles have attracted great interest in recent research because of their distinct electrical and mechanical properties, including high electrical conductivity, hardness, and others. Fullerene molecules are the basis for the construction of carbon nanotubes, because the ends of the carbon nanotubes are in the form of fullerene molecules [3]. Each carbon atom in the fullerene is aligned with three other carbon atoms and the positions of the carbon atoms in the fullerene molecule ( $C_{60}$ ) are identical and are located at a fixed distance from the centre of the molecule (approximately 3.55 Å) and the average distance between each two adjacent carbon atoms of 1.44 Å and the fullerene ( $C_{60}$ ) can be counted as a coiled graphite layer that generates a symmetric polyhedral shape consisting of 20 hexagonal rings and 12 pentagonal rings needed to form curved surfaces and this agrees with Euler's theorem. The carbon nanotubes are originally bi-directional strips of graphene wrapped around a specific axis to form a cylindrical shape with a diameter ranging between 50–0.4 nm, each carbon atom hybrid ( $sp^2$ ) has three covalent bonds with three other carbon atoms, and the fourth electron is in unhybridized orbital  $\pi$ , and since the unit cell in graphene includes two atoms, there will be even numbers of electrons that can give the conductor or semiconductor properties of carbon nanotubes [4].

Different techniques have been used in the preparation of carbon nanotube such as hot-filament chemical vapour deposition (HF-CVD) [5–7], thermal chemical vapour deposition [8, 9], plasma-enhanced chemical vapour deposition (PECVD) [10, 11], and laser ablation technique [12, 13].

In this study, different thickness of carbon nanolayers (30.5, 52.6 and 70.12 nm) have been used in the preparation of Si-CNT solar cell, carbon layers were examined using scanning electron microscope and measure the effect of the layer thickness and light in-

tensity on the solar cell out power.

Absorbance and transmittance index spectrum exhibits steady values for all concentrations along the range 300–550 nm before decreasing over the range 550–600 nm. The band gap was of 2.7 eV for the initial concentration, of 2.95 eV for the second concentration, and, finally, of 3.1 eV for the third concentration.

The structure of the films varies greatly throughout concentrations, as seen in scanning electron microscope images. X-ray spectrum show that the layers are crystalline completely, and peaks for all concentrations appear at the same  $2\theta$  with different intensities. In addition, the calculated grain size decreased with KOH concentration increasing.

Finally, the outcomes demonstrated the potential for producing a thin film from the semiconductor perovskite  $\text{CaZnO}_3$ , which makes it suitable for application in the production of solar cells and diodes.

## 2. EXPERIMENTAL METHOD

Carbon nanolayers have been deposited on silicon wafers to prepare Si-CNT junction using plasma-sputtering technique. The impurities expected to be formed on the surface of silicon strips can be divided into three categories, contamination fills, discreet particles and absorbed gas atoms, as a result of processing silicon strips during the preparation. In the process of cleaning the silicon wafers, chemical compounds are used as solvents for removing different types of impurities, and it includes a set of successive steps in which the silicon wafers is washed with distilled water for 2–3 minutes, washed with ethanol solution by ultrasonic for a period of 5–10 minutes, washed with distilled water for 2–3 minutes, washed with ultrasonic acetone solution for 5–10 minutes, washed with distilled water for 2–3 minutes and, then, immersed in HF hydrofluoric acid at a concentration of 9% for one minute to remove a layer of silicon dioxide generated as a result of oxidation, washed with distilled water for 2–3 minutes and finally immersed in acetone solution in order for the model to be dried directly [14, 15].

The plasma atomization technique was used to deposit a layer of carbon with different nanothicknesses 30.5, 52.6 and 70.12 nm of pure graphite columns (99.9%) in a vacuum chamber of  $10^{-2}$  mbar in an atmosphere of argon gas, the device used in the plasma atomization process is Q150R S/E/ES shown in Fig. 1.

The device-specific variables are determined by the thickness and structure of the carbon deposited layer, which can be controlled according to the amount of current passing through the carbon column, the time of pulses and the number of pulses, as shown in Table 1.

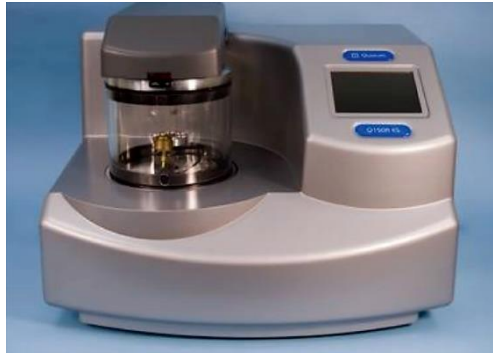


Fig. 1. Photograph of the Q150R S/E/ES plasma atomization system.

TABLE 1. Values of variables used in carbon deposition.

Parameter	Value
Material	Carbon
Pulse current	70 A
Pulses length	10 seconds
Number of pulses	5
Out gas time	60 second
Out gas current	50 A

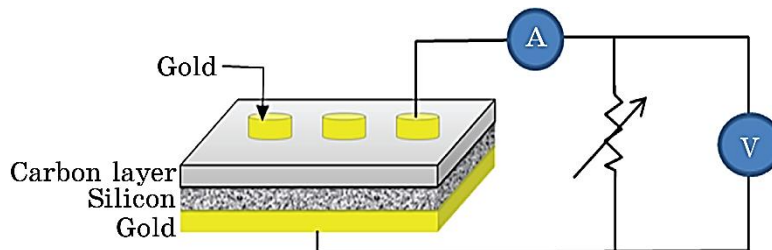


Fig. 2. Samples structure and the circuit used for measurement.

TABLE 2. Values of variables used in gold deposition.

Parameter	Value
Material	Gold
Sputter current	70 A
Terminate thickness	70 nm
Tooling factor	5
Out gas time	30 second
Out gas current	50 A

Gold was used as the electrode for the Si-CNT junction; layers of gold were deposited on the top and back surfaces of the junction to measure the electrical properties as shown in Fig. 2. The variables used in gold deposition shown in Table 2.

### 3. RESULTS AND DISCUSSION

Silicon wafers (*p*-type) have been used as a substrate to deposit different thickness of carbon nanolayers 30.5, 52.6 and 70.12 nm in the preparation of silicon-carbon nanotube junction Si-CNT; carbon layers have been examined using scanning electron microscope, and the effects of both the layer thickness and the light intensity on the solar cell out power were investigated.

Figure 3 show the scanning electron microscope (SEM) images of the carbon layers. The images showed aggregates of carbon nanoparticles, which took the form of clusters, and also showed a slight change in the size of the grains with the change in the thickness of the carbon layer, this is due to the fact that the plasma during the deposition process scrapes the carbon layer as a result of the proximity of the samples surfaces to the plasma, which will negatively affect the growth of the grains [17].

The effect of light intensity on the out power of the Si-CNT solar cell with different concentrations of carbon layer is shown in Fig. 3. The junction for all thicknesses behaves as a semiconductor of type *n* and this proves that the carbon nanotubes are of the multiwalled type because this type of tubes always behaves as a semiconductor [18]. The short circuit current and open circuit voltage

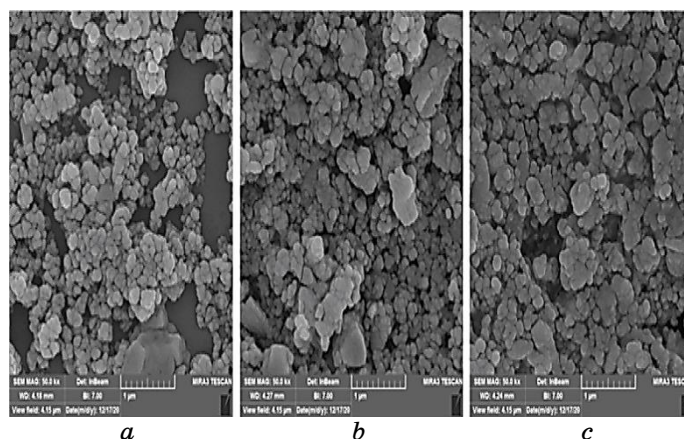
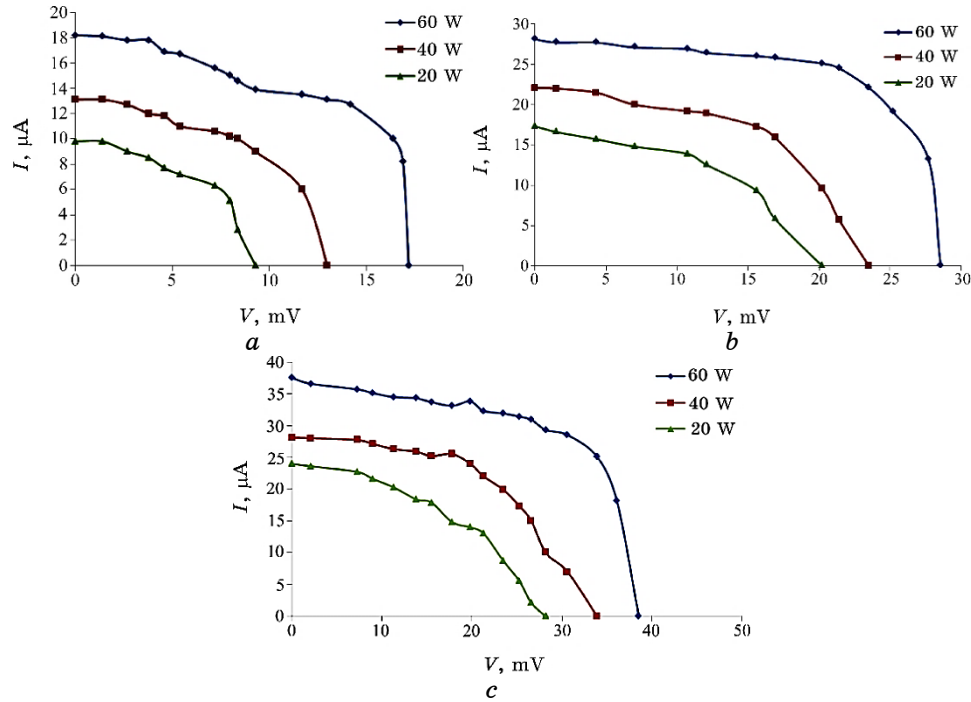


Fig. 3. Scanning electron microscope images of carbon layers with different thicknesses: *a*—30.5 nm; *b*—52.6 nm; *c*—70.12 nm.



**Fig. 4.** The out power of the Si-CNT solar cells with different carbon light intensities (20, 40 and 60W) and layers thicknesses: *a*—30.5 nm; *b*—52.6 nm; *c*—70.12 nm.

**TABLE 3.** Solar cell fill factor and efficiency with different carbon light intensities and layers thicknesses.

Thick, nm	Power, W	$I_{sc}$ , $\mu\text{A}$	$V_{oc}$ , mv	$FF$	$\eta$
30.5	60	18.2	17.2	0.576	0.30
	40	13.1	13	0.493	0.13
	20	9.8	9.3	0.497	0.075
52.6	60	28.1	28.55	0.653	0.87
	40	22.1	23.5	0.519	0.45
	20	17.3	20.2	0.432	0.25
70.12	60	37.5	38.55	0.603	1.45
	40	28.1	33.9	0.498	0.79
	20	24	28.2	0.389	0.43

increases for all thicknesses of carbon layers as a result of the increase of carbon nanotube density as shown in Fig. 4 and Table 3.

The effect of thickness on the Si-CNT solar cell is shown in Fig. 5; the out power of the Si-CNT junction (at a constant light inten-

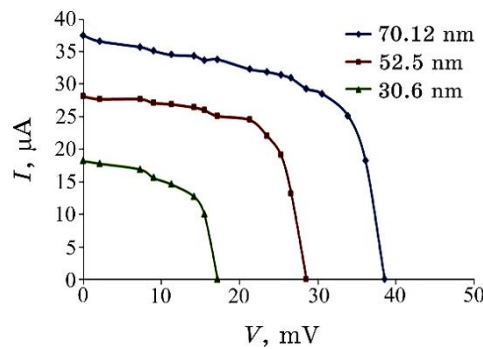


Fig. 5. The out power of Si-CNT solar cell with different carbon layer thickness.

sity of 60 W) increases with carbon layer thickness. The efficiency also increases with carbon layer thickness from 0.3 for the carbon layers with thickness of 30.5 nm to 0.87 for the carbon layers with thickness of 52.6 nm and, then, the efficiency becomes 1.45 for the carbon layers with thickness of 70.12 nm. This increase in efficiency with the thickness of the carbon layer could be due to the increase in the density of the carbon nanotubes as shown in Table 3.

#### 4. CONCLUSIONS

The carbon nanotubes have been constructed on a *p*-type silicon wafer substrates without catalysts. Scanning electron microscope showed that the grain size increases slightly with layer thickness. The Si-CNT junction behaves as a solar cell; the out power and efficiency increases with carbon layer thickness and light intensity.

#### REFERENCES

1. Timothy D. Burchell, *Carbon Materials for Advanced Technologies* (The Boulevard-Langford Lane Kidlington-Oxford, UK: Elsevier Science Ltd 0x5 IGB: 1999).
2. Andreas Hirsch, *Nature Materials*, **9**: 868 (2010).
3. T. Pradeep, *Nano: The Essential, Understanding the Nanoscience and Nanotechnology* (New Delhi: Tata McGraw-Hill Publishing Company Limited: 2007).
4. Daniel Jay Hornbaker, *Electronic Structure of Carbon Nanotube Systems Measured with Scanning Tunneling Microscopy* (Ph.D. Thesis in Physics (Graduate College of the University of Illinois at Urbana-Champaign: 2003).
5. Edward H. Wahl, *Laser-Based Diagnostics of Diamond Synthesis Reactors* (Report No. TSD-136, The U.S. Department of Energy Basic Energy Sciences) (Stanford, California: Stanford University: 2001).

6. E. N. Ganesh, *International Journal of Innovative Technology and Exploring Engineering (IJITEE)*, **2**, Iss. 4: 311 (2013).
7. E. N. Farabaugh, A. Feldman, and L. Robins, *2<sup>nd</sup> International Conference on the New Diamond Science and Technology* (Gaithersburg: National Institute of Standards and Technology, Ceramics Division: 1991), MD 20899.
8. Jurg Furer, *Growth of Single-Wall Carbon Nanotubes by Chemical Vapor Deposition for Electrical Devices* (Ph.D. Thesis) (Philosophisch-Naturwissenschaftlichen, Universitat Basel: 2006).
9. M. Daenen, R. D. de Fouw, B. Hamers, P. G. A. Janssen, K. Schouteden, M. A. J. Veld, *The Wondrous World of Carbon Nanotubes. 'A Review of Current Carbon Nanotube Technologies'* (Phillips NAT-lab–Eindhoven University of Technology: 2003).
10. Andrea Szaby, Caterina Perri, Anita Csaty, Girolamo Giordano, Danilo Vuono, and János B. Nagy, *Materials*, **3**: 3092 (2010); <https://doi.org/10.3390/ma3053092>
11. Todd Steiner, *Semiconductor Nanostructures for Optoelectronic Applications* (Boston–London: Artech House Inc.: 2004).
12. C. D. Scott, S. Arepalli, P. Nikolaev, and R. E. Smalley, *Materials Science & Processing, Appl. Phys.*, **A72**: 573 (2001); <https://doi.org/10.1007/s003390100761>
13. Muhammad Musaddique, Ali Rafique, and Javed Iqbal, *Journal of Encapsulation and Adsorption Sciences*, **1**: 29 (2011); <https://doi.org/10.4236/jeas.2011.12004>
14. Werner Kern, *J. Electrochem. Soc.*, **137**, No. 6: 1887 (1990); <https://doi.org/10.1149/1.2086825>
15. *Wet-Chemical Etching and Cleaning of Silicon* (Virginia Semiconductor Inc.: 2003).
16. Mohammad M. Uonis, Bassam M. Mustafa, and Anwar M. Ezzat, *World Journal of Nano Science and Engineering*, **4**, No. 2: 90 (2014); [doi:10.4236/wjnse.2014.42012](https://doi.org/10.4236/wjnse.2014.42012)
17. Mohammad M. Uonis, Bassam M. Mustafa, and Anwar M. Ezzat, *World Journal of Nano Science and Engineering*, **4**, No. 3: 105 (2014); [doi:10.4236/wjnse.2014.43014](https://doi.org/10.4236/wjnse.2014.43014)
18. M. S. Dresselhaus, G. Dresselhaus, and R. Saito, *Carbon*, **33**, No. 7: 883 (1995); [https://doi.org/10.1016/0008-6223\(95\)00017-8](https://doi.org/10.1016/0008-6223(95)00017-8)